JACS
JOURNAL OF THE AMERICAN CHEMICAL SOCIETY

ARTICLE

pubs.acs.org/JACS

Metallic Few-Layered VS_2 Ultrathin Nanosheets: High Two-Dimensional Conductivity for In-Plane Supercapacitors

Jun Feng,[†] Xu Sun,[†] Changzheng Wu,[*,†] Lele Peng,[†] Chenwen Lin,[†] Shuanglin Hu,[‡] Jinlong Yang,[†] and Yi Xie[*,†]

[†]Hefei National Laboratory for Physical Sciences at the Microscale, University of Science & Technology of China, Hefei, Anhui, 230026, P.R. China

[‡]Shanghai Supercomputer Center, Shanghai, 201203, P.R. China

Supporting Information

ABSTRACT:

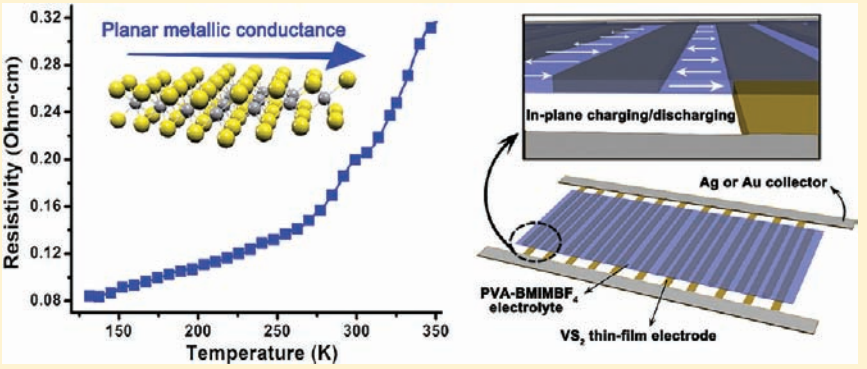

With the rapid development of portable electronics, such as e-paper and other flexible devices, practical power sources with ultrathin geometries become an important prerequisite, in which supercapacitors with in-plane configurations are recently emerging as a favorable and competitive candidate. As is known, electrode materials with two-dimensional (2D) permeable channels, high-conductivity structural scaffolds, and high specific surface areas are the indispensible requirements for the development of in-plane supercapacitors with superior performance, while it is difficult for the presently available inorganic materials to make the best in all aspects. In this sense, vanadium disulfide (VS_2) presents an ideal material platform due to its synergic properties of metallic nature and exfoliative characteristic brought by the conducting S−V−S layers stacked up by weak van der Waals interlayer interactions, offering great potential as high-performance in-plane supercapacitor electrodes. Herein, we developed a unique ammonia-assisted strategy to exfoliate bulk VS_2 flakes into ultrathin VS_2 nanosheets stacked with less than five S−V−S single layers, representing a brand new two-dimensional material having metallic behavior aside from graphene. Moreover, highly conductive VS_2 thin films were successfully assembled for constructing the electrodes of in-plane supercapacitors. As is expected, a specific capacitance of 4760 μF/cm^2 was realized here in a 150 nm in-plane configuration, of which no obvious degradation was observed even after 1000 charge/discharge cycles, offering as a new in-plane supercapacitor with high performance based on quasi-two-dimensional materials.

INTRODUCTION

Layered transition-metal dichalcogenides (TMDs), such as MoS_2, WS_2, and VS_2 etc., have been successfully established as a new paradigm in the chemistry of nanomaterials especially for nanotubes and fullerene-like nanostructures as well as the graphene analogues during the past decades.[1−4] From the structural point of view, vanadium disulfide (VS_2) is a typical family member of TMDs, in that VS_2 crystals are composed of the metal V layers sandwiched between two sulfur layers and stacked together by weak van der Waals interactions.[5] However, since the first discovery of VS_2 in 1970s, rigid high-temperature solid-state processes under H_2S atmosphere were inevitably required for the formation of VS_2 in the previously reported synthetic approaches, which provided practical difficulties for scientists to investigate this material, resulting in the long term absence of systematic research works on VS_2 in both academic and industrious areas.[6,7] Nevertheless, the unique and complicated electronic structure of VS_2 inspired us that this layered compound deserves specific attention as a promising functional material, since the 2D electron−electron correlations among V atoms would preferably induce more complicated planar electric transportation properties.[8]

As is rapidly emerging recently, quasi-two-dimensional materials have provided new opportunities to satisfy people's requirements of ultrathinness, transparency, and flexibility in high-level

Received: July 31, 2011
Published: September 27, 2011

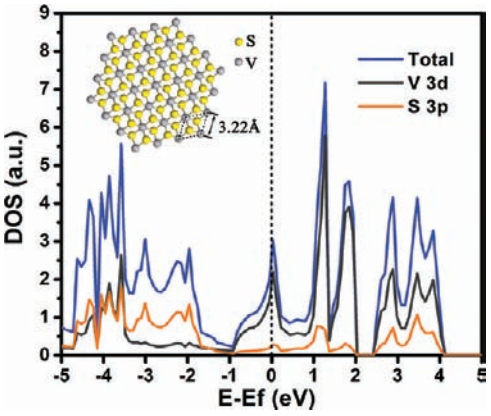

Figure 1. DOS diagram for single-layered VS_2 calculated by Heyd−Scuseria−Ernzerhof (HSE) hybrid functional, revealing the 2D metallic nature of VS_2 single layers. Inset is the *c*-axis projected atomic view of S−V−S, a single layer structural lattice.

integrated electronic systems, in that two-dimensionality could provide the bridge to combine microscopic compressibility (for integration) with macroscopic extensibility (for operation), guaranteeing a maximum functionality while keeping the size minimized.[9−11] In this regard, the most typical 2D material platforms are based on graphene and its derivative materials.[12,13] Especially, graphene-based in-plane supercapacitor, i.e., building each two electrodes onto the same plane (or surface), is newly emerging as a noteworthy and promising candidate for next-generation energy-storage devices.[14−18] Considering that in-plane supercapacitor designs call for electrodes with 2D permeable channels, which were actually quite limited in the presently available materials, the development of new material platforms to fabricate planar energy storage devices becomes an indispensible and challenging task.

Although graphene has demonstrated outstanding performance as the electrodes of in-plane supercapacitors, the improvement of electric conductivity for large-area graphene thin films at low cost is actually still a demanding work.[19] In this sense, aside from further improving of graphene materials, new alternatives should be developed as complementary approaches toward thinner and better supercapacitors. A favorable choice lies in the inorganic graphene analogues (IGAs), i.e., the mono- or few-layered nanosheets exfoliated from layered compounds with weak interlayer interactions, which have attracted tremendous attention due to the more complicated and diversified electronic structures of inorganic compounds than that of all-carbon materials.[4,10] However, the conventional IGAs were semiconducting (MoS_2 and WS_2) or insulating (BN and BCN), of which the relatively low conductivity substantially hampered them from being utilized as supercapacitor electrode materials.[20,21]

As is known, with regard to the evaluation of electrode material in supercapacitors, conductivity and specific surface area are two critical factors determining the supercapacitor performances.[14] Intriguingly, our theoretical investigations reveal that the monolayered structure of VS_2 is of metallic behavior in which the density of states (DOS), see Figure 1, resides across the Fermi level with high local DOS values, presenting promising sign for high microscopic 2D conductivity.[5] Moreover, the weak van der Waals interlayer interaction gives the practical feasibility for VS_2 to be exfoliated into ultrathin nanosheets with high surface activity, just as the exfoliation of graphite into graphene.[22] Therefore, in view of the advantages of 2D conducting materials for planar energy storage devices, VS_2 nanosheets with high electric conductivity would be of high interest and of significance for the fabrication of planar supercapacitors.

The formation of a VS_2 phase greatly suffered from the inconvenient and toxic synthetic methodologies during the past decades, let alone the realization of well-dispersed high-quality VS_2 ultrathin nanosheets. Herein, we highlight an all-in-solution route to synthesize VS_2 phase for the first time, taking advantage of an intermediate intercalated compound precursor of $VS_2 \cdot NH_3$. In our case, the high-dispersing capability of the in-solution prepared samples ensured us to successfully exfoliate NH_3-intercalated $VS_2 \cdot NH_3$ into VS_2 ultrathin nanosheets with less than five S−V−S atomic layers, representing a brand new inorganic 2D material having metallic behavior aside from graphene. Furthermore, inspired by the planar metallic nature of VS_2 nanosheets, a highly *c*-oriented VS_2 thin film with synergic advantages of high conductivity and high specific area was assembled by vacuum filtration from the as-exfoliated nanosheets, of which the double-layered capacitive properties were characterized in an in-plane configuration. As is expected, this highly conductive VS_2 thin film demonstrated a high specific capacitance, showing promising signs for this new 2D material to be utilized in energy storage devices.

EXPERIMENTAL SECTION

Materials. Sodium orthovanadate ($Na_3VO_4 \cdot 12H_2O$), thioacetamide (TAA), and formamide were commercially available from Shanghai Chemical Reagent Co. Ltd. All reagents were analytical grade and used as received without further purification.

Preparation of $VS_2 \cdot NH_3$ Precursor. In a typical experiment, 3 mmol $Na_3VO_4 \cdot 12H_2O$ and 15 mmol TAA were dissolved in 40 mL distilled water in a glass jar, which was then stirred for 1 h to form a homogeneous solution and transferred to a 50 mL Teflon-lined autoclave. The autoclave was sealed and heated at 160 °C for 24 h. Afterward, the system was allowed to cool down to room temperature. Black precipitate was finally collected by centrifugation and washed several times with distilled water. Of note, the obtained precursor should be instantly used in the following exfoliation procedures without being dried, otherwise the $VS_2 \cdot NH_3$ would decompose into VS_2 flakes and result in lower exfoliation efficiency, as is compared in Figure S7, Supporting Information.

Exfoliation of the Precursor into VS_2 Nanosheets. In our experiment, 20 mg $VS_2 \cdot NH_3$ was dispersed in a conical flask with 30 mL water and then bubbled with argon to expel the dissolved oxygen away from the solution, avoiding the possible oxidation of V(IV) to V(V). Then the above dispersion was ultrasonicated in iced water for 3 h. The resultant black suspension was filtered by a medium-speed qualitative paper filter to remove the unexfoliated flakes from the solution, resulting in a translucent solution of VS_2 nanosheets.

Assembly of VS_2 Nanosheets into Transferrable Thin Films. VS_2 nanosheet solution was vacuum filtrated over a cellulose membrane with 0.22 μm pore size to form a homogeneous thin film, of which the thickness can be tuned by changing the filtrated amount of VS_2 nanosheet solution. X-ray diffraction (XRD) was employed to reveal the orientation of this restacked $VS_2 \cdot NH_3$ film.

Device Fabrication of In-Plane Supercapacitor. The prototype device of the VS_2 nanosheet-based in-plane supercapacitor was fabricated by a mechanical shaping process modified from the previous method adopted to fabricate graphene-based in-plane supercapacitors.[18] In brief, a series of blades were stacked side by side accurately as the mold for creating plentiful VS_2 ribbons with micrometer-scale gaps. Au charge

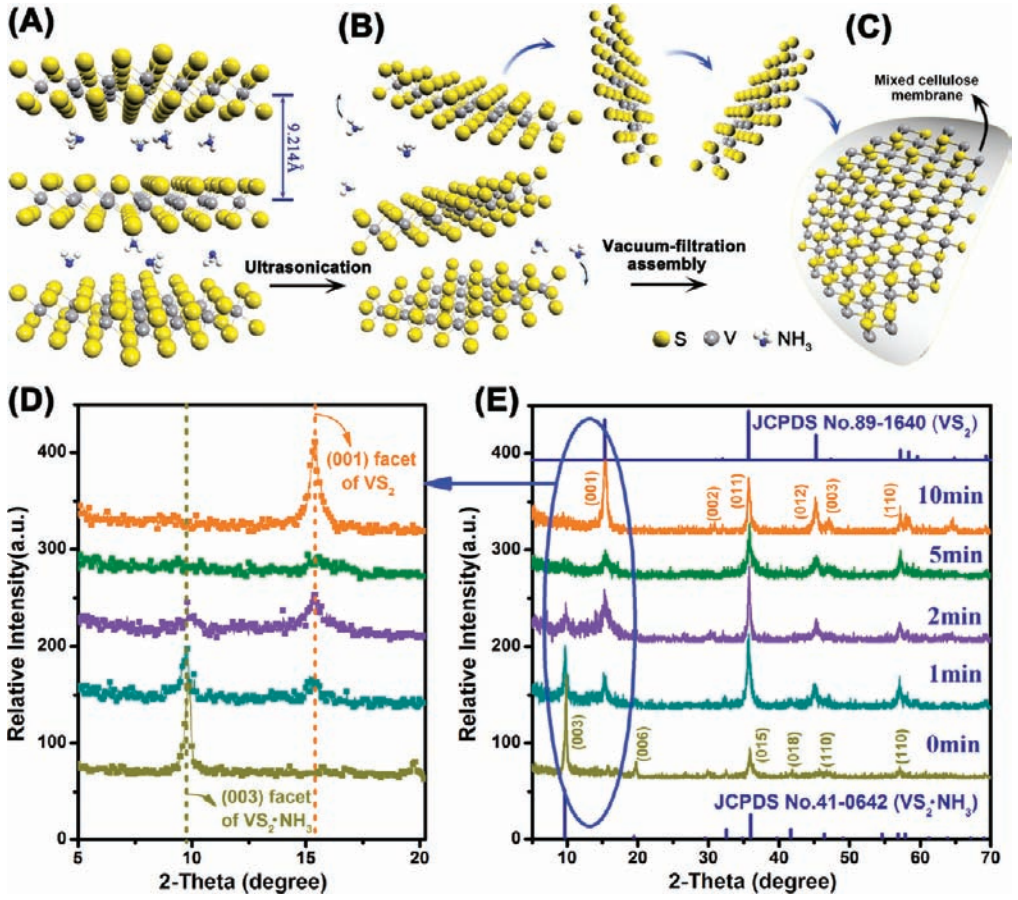

Figure 2. (A) The $VS_2 \cdot NH_3$ precursor with NH_3 molecules intercalated into the S−V−S layers. (B) Effusion of NH_3 molecules away from the stacked layers, breaking down the *c* axis periodicity and resulting in the formation of ultrathin VS_2 nanosheets. (C) Vacuum-filtration assembly of the as-synthesized VS_2 nanosheets into transferrable thin films on mixed cellulose membrane. (D and E) Phase transformation analysis throughout the exfoliation process. (D) Magnified plots of the circled area in (E), which shows substantial shifts of the facet along *c* axis, indicating the gradual transformation of $VS_2 \cdot NH_3$ into VS_2. Of note, the samples were restacked and collected by high-speed centrifugation and fully grounded to avoid orientation for better phase identification.

collectors were deposited onto the VS_2 ribbons utilizing a specifically shaped mask. Finally, the overall compact device was fabricated after spread $BMIMBF_4$−PVA electrolyte coating onto the ribbon-shaped electrodes, as shown in Figure 5B.

Characterize. XRD was performed on a Philips X'Pert Pro Super diffractometer with Cu Kα radiation (λ = 1.54178 Å). The transmission electron microscopy (TEM) images were obtained on a JEOL-2010 transmission electron microscope at an acceleration voltage of 200 kV. The field emission scanning electron microscopy (FE-SEM) images were taken on a JEOL JSM-6700F SEM. High-resolution TEM (HR-TEM) images were taken on a JEOL 2010 microscope at an accelerating voltage of 200 kV. Electrochemical performance of the supercapacitor was studied in a two-electrode system by cyclic voltammetry (CV) and galvanostatic charge/discharge at an electrochemical station (CHI660B). The scan rate of the CV response varied from 20 to 200 mV/s with the potential range of −0.6 to 0.6 V. Potential range set for galvanostatic charge/discharge tests was 0.02−0.6 V.

Calculation Details. The electronic structure calculations of bulk and monolayer VS_2 were performed using the projector augmented wave (PAW) method with the Perdew−Burke−Ernzerhof (PBE) generalized gradient approximation (GGA) functional and Heyd−Scuseria−Ernzerhof (HSE) hybrid functional as recently implemented in VASP code.[23−25] The geometry structures were adopted from experimental XRD measurements without relaxation. For the monolayer VS_2, the lattice parameter in the *c* direction was set to 4 times that of the *c* value in bulk, thus the thickness of vacuum layer is about 20 Å. The energy cutoff for plane-wave basis expansion was set to 500 eV. The total energies were calculated by both PBE and HSE functionals with the convergence criteria 1×10^{-5} eV per unit cell. Gamma-centered *k*-points grids $8 \times 8 \times 4$ and $8 \times 8 \times 1$ were sampled with Monkhorst Pack method for bulk and monolayer VS_2, respectively. For the DOS calculations, denser *k*-points grids of $14 \times 14 \times 8$ and $14 \times 14 \times 1$ were used.

RESULTS AND DISCUSSION

As a complementary research area of graphene, inorganic quasi-2D materials have attracted widespread attention of both chemists and physicists. Traditionally, IGAs were synthesized by the exfoliation of layered compounds through intercalation−exfoliation processes. For example, MoS_2 and WS_2 graphene analogues were obtained by lithium intercalation followed by in-water exfoliation;[4] hexagonal nickel hydroxide nanosheets were synthesized by exfoliating layered nickel hydroxide intercalated with dodecyl sulfate ions,[26] and the soft-chemical exfoliation of layered molybdenum oxide into MoO_2 nanosheets was reported to be realized by ion exchanging between H^+ and TBA^+.[27] However, most of these processes required the insertion

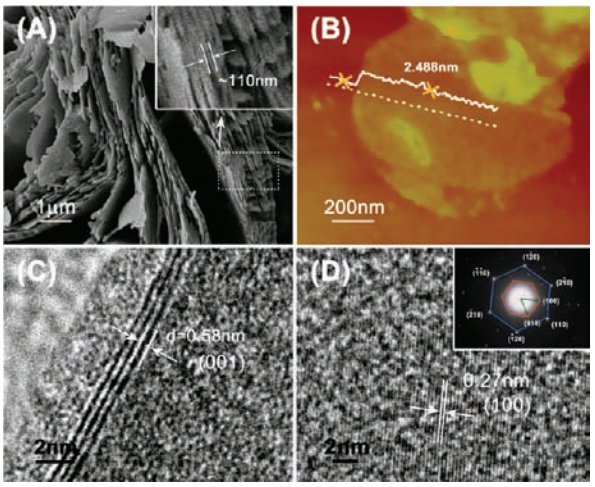

Figure 3. (A) SEM image of the precursor $VS_2 \cdot NH_3$, in which a flake thickness of about 110 nm was measured. (B) Tapping mode AFM image of the exfoliated VS_2 nanosheets, showing a thickness of only 3 nm, which indicates that the precursor has indeed been successfully exfoliated into ultrathin nanosheets with only a few stacked atomic layers. (C and D) HR-TEM and SA-ED analysis of the as-obtained VS_2 nanosheets, in which each facets of (001) and (100) can be well indexed. Also, microscopic *c* orientation could be observed according to the SA-ED pattern with hexagonal symmetry shown in the inset of (D).

of nonvolatile ions to swell the layers, which sometimes was quite unfavorable when fabricating practical nanodevices in that the surface residue of foreign ions was usually not easy to be thoroughly removed, leading to the instability or changing of surface properties. Ammonia (NH_3) is a micromolecule with very positive physical activity and chemical reactivity, of which the volatile characteristic inspired us to exfoliate NH_3-intercalated VS_2, so there would be no residue of foreign ions in the assembled structures after the evaporation of NH_3. Taking advantage of an unstable precursor formulated as $VS_2 \cdot NH_3$, this design of rational synthesis and assembly was successfully realized. In brief, $VS_2 \cdot NH_3$ was hydrothermally prepared by reacting two common raw materials of ammonium metavanadate (NH_4VO_3) and thioacetamide (TAA), in which TAA was chosen to serve as the chemical source of both ammonia and sulfide, as is discussed in S5, Supporting Information. The precursor was ultrasonically treated in water, resulting in the fully exfoliation of bulk $VS_2 \cdot NH_3$ into ultrathin VS_2 nanosheets with the effusion of NH_3. Afterward, VS_2 thin film was assembled by a vacuum-filtration method, as was previously adopted to fabricate flexible graphene films.[28,29] The overall experimental procedure was schematically illustrated in Figure 2A–C.

By XRD phase analysis, the intermediate states throughout the reaction were investigated, as is shown in Figure 2D,E. Samples with different sonication times were collected by centrifuging the dispersion and grounded to avoid possible orientation for better phase identification. The results clearly show that $VS_2 \cdot NH_3$ can be rapidly transformed into VS_2 within 10 min, and the product is single-phased VS_2 without noticeable degradation of S–V–S layers. Figure 2D is the magnification of the circled area in Figure 2E. As can be seen, the (003) peak of $VS_2 \cdot NH_3$ at 9.59° gradually shifted to the (001) peak of VS_2 at 15.38°, indicating the reduction of S–V–S interlayer spacing from 9.21 to 5.73 Å. The difference between these two interlayer spacing (~3.5 Å) was consistent with the hydrogen-bonding diameter (~3.6 Å) of NH_3 in metal disulfides,[30] confirming that NH_3 molecules were loosely attached to each S–V–S layers by weak van der Waals force and hydrogen bonds, which determined the exfoliative nature of $VS_2 \cdot NH_3$ and facilitated the evolution toward VS_2 nanosheets. On the other hand, the exfoliation process was conducted in aqueous environment, in which the strong hydrogen bonds between NH_3 and H_2O molecules further promoted the effusion of NH_3 away from bulk $VS_2 \cdot NH_3$, destroying the periodicity along the *c* axis.

To better understand the NH_3-assisted exfoliation process and the final products, microscopic investigations were performed to study the morphological transformation from $VS_2 \cdot NH_3$ to VS_2. Figure 3A shows the SEM image of the precursor $VS_2 \cdot NH_3$, showing a typical layered structure stacked layer by layer. The magnified image as shown in the inset of Figure 3A revealed that the thickness of $VS_2 \cdot NH_3$ flakes was about 110 nm. For comparison, tapping mode atomic force microscopy (AFM) image of the VS_2 nanosheet product exfoliated from $VS_2 \cdot NH_3$ flakes is shown in Figure 3B. Prominently, the thickness was measured to be only 3.0 nm, which was more than 35 times thinner than that of the precursor, indicating the successful production of ultrathin VS_2 nanosheets as a new graphene analogue. Furthermore, considering that the *c* parameter of VS_2 is 5.73 Å, the thickness of 2.488 nm denoted that the product was comprised of 4–5 single layers of S–V–S. HR-TEM investigation in the edge areas of ultrathin sample was a common and direct method to determine the layer numbers microscopically.[31,32] In our case, as is presented in Figure 3C, four to five dark and bright patterns can be readily identified, indicating that the sample was stacked up with four to five single layers, which was in accordance with the results measured by AFM. Moreover, the interlayer spacing measured in the edge-area HR-TEM image was about 0.58 nm, which was also in accordance with the c parameter of VS_2 (0.573 nm). Of note, the majority of the VS_2 nanosheets observed by HR-TEM were *c* oriented, since the selected area electron diffraction (SA-ED) patterns (inset of Figure 3D) of them mostly presented well-defined hexagonal symmetry. HR-TEM image projected along *c* axis is shown in Figure 3D, in which the interplanar spacing was measured to be 0.27 nm according to the periodic pattern in the lattice fringe image, matching up with that of the (100) facet of VS_2 (2.784 Å). These results clearly demonstrated that the $VS_2 \cdot NH_3$ flakes were successfully exfoliated into ultrathin nanosheets with good quasi-2D crystallinity and microscopic orientation along *c* axis, providing the prerequisite for further assembly of this material into large-area practical devices.

Assembly and transfer of ultrathin materials into large-area thin films, such as graphene films, is an essential process for device fabrication, particularly in flexible electronics.[33–35] In order to assemble the as-synthesized VS_2 nanosheets into large-scale compact thin films, we adopted the vacuum-filtration method as was commonly applied for the assembly of graphene thin films.[28] Briefly, the as-ultrasonicated VS_2 nanosheet dispersion was allowed to stand still for 10 h, after which the one-third supernatant of the as-obtained VS_2 nanosheet dispersion was decanted into another container in order to remove the unexfoliated flakes. The decanted nanosheet dispersion was then diluted, ultrasonically treated again for 30 min, and vacuum-filtrated onto a mixed cellulose membrane with the pore size of 0.22 μm, forming a gray to black homogeneous thin film on the membrane, of which the thickness can be well controlled by tuning the filtrated volume of the dispersion, as is demonstrated

in Figure 4A. The obtained VS_2 thin film on cellulose membrane can be readily transferred onto arbitrary surfaces by dissolving the membrane substrate, as is schematically presented in Figure S6, Supporting Information. As a consequence of the microscopic self-orientation of quasi-2D VS_2 nanosheets, the transferred thin film assembled by this method was also highly *c* oriented, as is revealed by the XRD analysis shown in Figure 4B, in that only the peak of (001) facet can be detected. To confirm the theoretically expected planar metallic conductance as is discussed above, temperature dependence of the planar resistivity of the as-obtained thin film was carried out, of which the result is shown in Figure 4C. As can be seen, with the increasing of temperature, an increasing response of electric resistivity was observed, showing the typical metallic conducting behavior and confirming the metallicity of VS_2 nanosheets.[5] Of note, when transferred onto flexible substrates, the as-assembled thin film presented a very high endurance toward bending. Figure 4D demonstrated that the conductivity only shows a very small degradation even after 200 bending cycles. This high mechanical endurance provides promising signs for this highly conductive thin film to be utilized in flexible electronics, especially for the electrode materials of energy-related devices, such as lithium-ion batteries, schottky solar cells, and supercapacitors with high flexibility.[27]

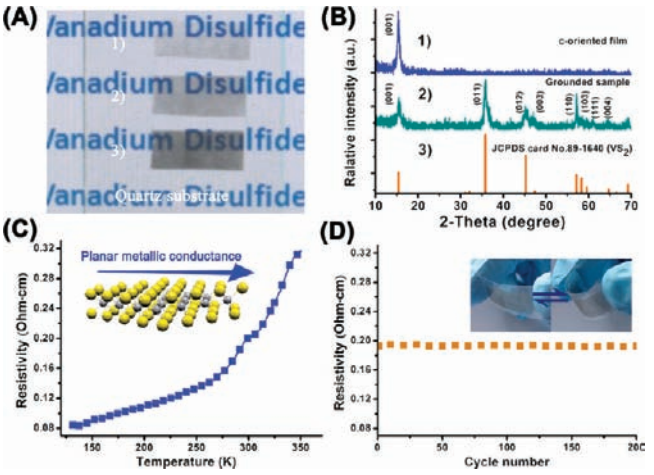

Figure 4. (A) Demonstration of the VS_2 thin films with different thickness transferred onto a quartz substrate, showing translucent feature. (B) Well-defined *c* orientation observed by the XRD pattern of the as-assembled VS_2 thin film. (C) Temperature dependence of planar resistivity of VS_2 thin film. (D) Demonstration of the conductance stability for a ribbon-shaped electrode fabricated from the VS_2 thin film under repeated bending/extending deformation.

To demonstrate the promising application of the as-obtained highly conductive thin film assembled from VS_2 nanosheets, we fabricated a supercapacitor with this film in a recently developed all-in-plane configuration, which is widely believed to be efficient in the minimizing of overall thickness and the maximizing of electrode utilization for the power source of next-generation electronic devices.[17,18] The main feature of this supercapacitor is that the device can be built onto arbitrary surfaces with minimized thickness, while keeping a reasonable electric capacitance, as is illustrated in Figure 5A. Given the fact that the transport of ions is parallel to the electrodes, the quasi-2D feature of VS_2 nanosheets is quite conducive to the charge/discharge processes, since the ions would not be blocked all along the transportation pathway inside the interlayer space between each two single layers.[18] To more compactly integrating this in-plane supercapacitor, here we used a solid-state polymer electrolyte prepared by mixing the polyvinylalcohol (PVA) gel with a water-soluble ionic liquid of $BMIMBF_4$, which was modified according to the literatures.[14,36,37]

Figure 5C−F are the electrochemical characterization results of the as-fabricated in-plane supercapacitor. Near-rectangular CV at different scanning rates were presented in Figure 5C, revealing the typical double-layer capacitor behaviors. No obvious redox

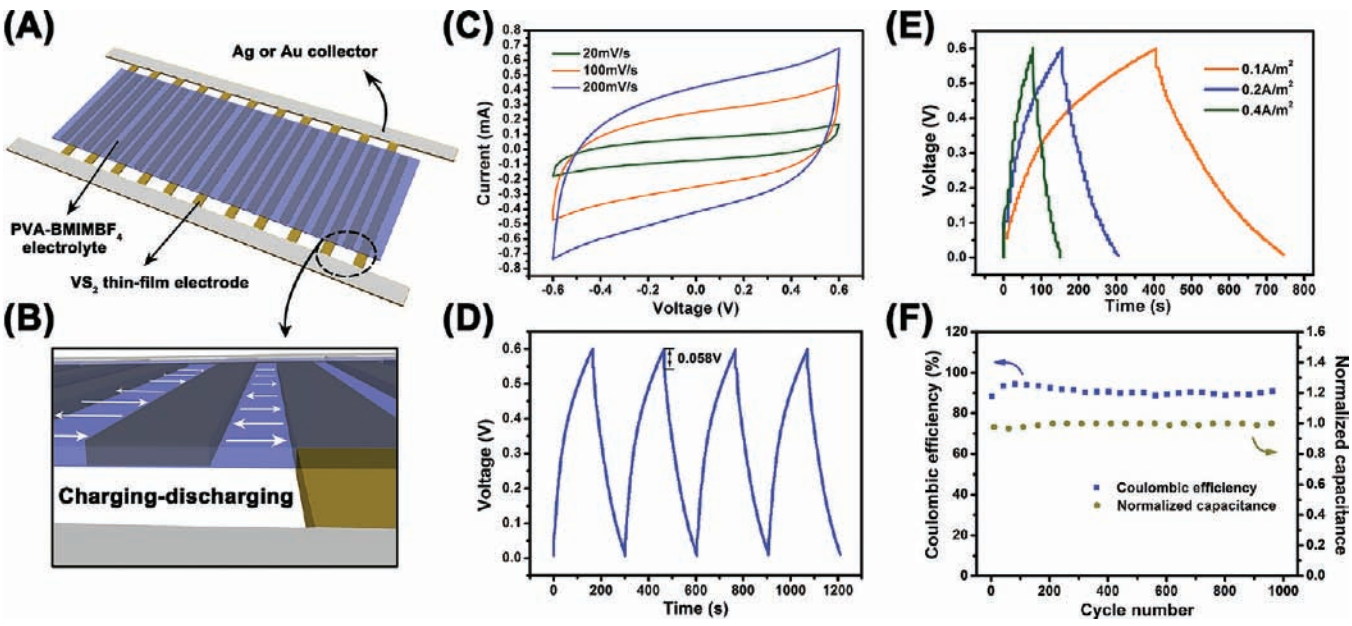

Figure 5. (A) Planar ion migration pathways for the in-plane supercapacitor. (B) Schematic illustration of the in-plane configuration of the as-fabricated supercapacitor. (C) CV at different scanning rates of 20, 100, and 200 mV/s. (D) Galvanostatic cycling behavior and IR drop illustration. (E) Galvanostatic charge/discharge curves of the as-fabricated in-plane supercapacitor. (F) Cycle life investigation of the supercapacitor, showing negligible degradations in the coulomb efficiency and specific capacitance.

peaks could be observed in the voltage range between −0.6 and 0.6 V, implying that pseudocapacitance had no contributions toward the VS_2 nanosheet supercapacitor fabricated here. Moreover, Figure 5D,E is the galvanostatic charge−discharge curves of the in-plane supercapacitor, from which the specific capacitance can be derived based on the following equation:[38,39]

$$C = I\frac{\Delta t}{A\Delta V}$$

where I is the applied working current, Δt represents the discharging time, ΔV is the voltage range, and A is the total electrode area. The thickness and geometric area of the electrode thin film was measured to be 150 nm and 11.52 cm^2, respectively. Accordingly, the as-fabricated supercapacitor had a specific capacitance of 4760 $\mu F/cm^2$ (i.e., 317 F/cm^3), which is comparable with the graphene-based supercapacitors in planar configurations (394 $\mu F/cm^2$ with a thickness of 10 nm, i.e., 394 F/cm^3).[18] Besides, considering that we did not blend any conductive additives into the VS_2 nanosheet electrodes, the IR drop of 0.058 V observed in Figure 5D implied a very small intrinsic series resistance inside the electrodes, which we believe should be attributed to the high conductivity brought by the metallic nature of VS_2 nanosheets. Also, as shown in Figure 5F, only a negligible degradation of capacitance was observed after 1000 charge/discharge cycles while keeping a coulomb efficiency of higher than 90%, revealing the excellent cycling behavior of the VS_2 nanosheet-based in-plane supercapacitor. The considerable specific capacitance, long cycle life, and ultrathin configuration provide the practical feasibility to bring the supercapacitors fabricated in this configuration into practice as the power sources of micro-/nano-sized electronic devices, while geometrically ultrathin energy-storage devices are urgently required nowadays to satisfy the rapid development of portable, flexible, and transparent electronics.[15]

CONCLUSION

Our developed new VS_2 graphene analogue with less than five S−V−S atomic layers can be applied directly to the assembly of highly *c* oriented VS_2 thin films with synergic advantages of high conductivity and 2D permeable channels, thereby opening the door to design practical in-plane supercapacitors for the power sources in advanced ultrathin electronics. Electrochemical characterization revealed a considerable specific electric capacitance of 4760 $\mu F/cm^2$ and an excellent cycling behavior even after 1000 charge/discharge cycles for this in-plane supercapacitor, providing theoretical and technical feasibility for it to be further improved and scaled up for the practical power source of intelligent devices. In this sense, developing new 2D material platforms with high conductivity paves a new way to construct practical power sources for the next-generation intelligent devices, especially those with ultrathin and mechanically endurable configurations.

ASSOCIATED CONTENT

Supporting Information. Supplementary characterizations, analysis of the formation of $VS_2 \cdot NH_3$ precursor, demonstration of the transferrable feature of the VS_2 thin film, and experimental details and comparisons for the exfoliation process. This material is available free of charge via the Internet at http://pubs.acs.org.

AUTHOR INFORMATION

Corresponding Author
yxie@ustc.edu.cn; czwu@ustc.edu.cn.

ACKNOWLEDGMENT

The authors acknowledge the financial support from the National Basic Research Program of China (no. 2009CB93-9901), National Natural Science Foundation of China (no. 11074229, 11079004, 10979047, 90922016, 11132009), and innovation project of Chinese Academy of Science (KJCX2-YW-H2O), Program for New Century Excellent Talents in University and Chinese Universities Scientific Fund (CUSF).

REFERENCES

(1) Coleman, J. N.; Lotya, M.; O'Neill, A.; Bergin, S. D.; King, P. J.; Khan, U.; Young, K.; Gaucher, A.; De, S.; Smith, R. J.; Shvets, I. V.; Arora, S. K.; Stanton, G.; Kim, H.-Y.; Lee, K.; Kim, G. T.; Duesberg, G. S.; Hallam, T.; Boland, J. J.; Wang, J. J.; Donegan, J. F.; Grunlan, J. C.; Moriarty, G.; Shmeliov, A.; Nicholls, R. J.; Perkins, J. M.; Grieveson, E. M.; Theuwissen, K.; McComb, D. W.; Nellist, P. D.; Nicolosi, V. *Science* **2011**, *331*, 568.

(2) Radisavljevic, B.; Radenovic, A.; Brivio, J.; Giacometti, V.; Kis, A *Nat. Nanotechnol.* **2011**, *6*, 147.

(3) Kaplan-Ashiri, I.; Cohen, S. R.; Gartsman, K.; Ivanovskaya, V.; Heine, T.; Seifert, G.; Wiesel, I.; Wagner, H. D.; Tenne, R. *Proc. Natl. Acad. Sci. U.S.A.* **2006**, *103*, 523.

(4) Ramakrishna Matte, H. S. S.; Gomathi, A.; Manna, A. K.; Late, D. J.; Datta, R.; Pati, S. K.; Rao, C. N. R. *Angew. Chem., Int. Ed.* **2010**, *49*, 4059.

(5) Mulazzi, M.; Chainani, A.; Katayama, N.; Eguchi, R.; Matsunami, M.; Ohashi, H.; Senba, Y.; Nohara, M.; Uchida, M.; Takagi, H.; Shin, S. *Phys. Rev. B* **2010**, *82*, 075130.

(6) Murphy, D. W.; Cros, C.; Di Salvo, F. J.; Waszczak, J. V. *Inorg. Chem.* **1977**, *16*, 3027.

(7) Therese, H. A.; Rocker, F.; Reiber, A.; Li, J.; Stepputat, M.; Glasser, G.; Kolb, U.; Tremel, W. *Angew. Chem., Int. Ed.* **2005**, *44*, 262.

(8) Katayama, N.; Uchida, M.; Hashizume, D.; Niitaka, S.; Matsuno, J.; Matsumura, D.; Nishihata, Y.; Mizuki, J.; Takeshita, N.; Gauzzi, A.; Nohara, M.; Takagi, H. *Phys. Rev. Lett.* **2009**, *103*, 146405.

(9) Pushparaj, V. L.; Shaijumon, M. M.; Kumar, A.; Murugesan, S.; Ci, L.; Vajtai, R.; Linhardt, R. J.; Nalamasu, O.; Ajayan, P. M. *Proc. Natl. Acad. Sci. U.S.A.* **2007**, *104*, 13574.

(10) Radisavljevic, B.; Radenovic, A.; Brivio, J.; Giacometti, V.; Kis, A. *Nat. Nanotechnol.* **2011**, *6*, 147.

(11) Service, R. F. *Science* **2009**, *324*, 875.

(12) Geim, A. K.; Novoselov, K. S. *Nat. Mater.* **2007**, *6*, 183.

(13) Kim, K. S.; Zhao, Y.; Jang, H.; Lee, S. Y.; Kim, J. M.; Kim, K. S.; Ahn, J. H.; Kim, P.; Choi, J. Y.; Hong, B. H. *Nature* **2009**, *457*, 706.

(14) Zhu, Y.; Murali, S.; Stoller, M. D.; Ganesh, K. J.; Cai, W.; Ferreira, P. J.; Pirkle, A.; Wallace, R. M.; Cychosz, K. A.; Thommes, M.; Su, D.; Stach, E. A.; Ruoff, R. S. *Science* **2011**, *332*, 1537.

(15) Chmiola, J.; Largeot, C.; Taberna, P. L.; Simon, P.; Gogotsi, Y. *Science* **2010**, *328*, 480.

(16) Miller, J. R.; Outlaw, R. A.; Holloway, B. C. *Science* **2010**, *329*, 1637.

(17) Pech, D.; Brunet, M.; Durou, H.; Huang, P.; Mochalin, V.; Gogotsi, Y.; Taberna, P. L.; Simon, P. *Nat. Nanotechnol.* **2010**, *5*, 651.

(18) Yoo, J. J.; Balakrishnan, K.; Huang, J.; Meunier, V.; Sumpter, B. G.; Srivastava, A.; Conway, M.; Mohana Reddy, A. L.; Yu, J.; Vajtai, R.; Ajayan, P. M. *Nano Lett.* **2011**, *11*, 1423.

(19) Bae, S.; Kim, H.; Lee, Y.; Xu, X.; Park, J. S.; Zheng, Y.; Balakrishnan, J.; Lei, T.; Ri Kim, H.; Song, Y. I.; Kim, Y. J.; Kim, K. S.; Ozyilmaz, B.; Ahn, J. H.; Hong, B. H.; Iijima, S. *Nat. Nanotechnol.* **2010**, *5*, 574.

(20) Nag, A.; Raidongia, K.; Hembram, K. P. S. S.; Datta, R.; Waghmare, U. V.; Rao, C. N. R. *ACS Nano* **2010**, *4*, 1539.
(21) Rao, C. N. R.; Nag, A. *Eur. J. Inorg. Chem.* **2010**, *27*, 4244.
(22) Tang, Z.; Zhuang, J.; Wang, X. *Langmuir* **2010**, *26*, 9045.
(23) Blöchl, P. E. *Phys. Rev. B* **1994**, *50*, 17953.
(24) Perdew, J. P.; Burke, K.; Ernzerhof, M. *Phys. Rev. Lett.* **1996**, *77*, 3865.
(25) Heyd, J.; Scuseria, G. E.; Ernzerhof, M. *J. Chem. Phys.* **2003**, *118*, 8207.
(26) Ida, S.; Shiga, D.; Koinuma, M.; Matsumoto, Y. *J. Am. Chem. Soc.* **2008**, *130*, 14038.
(27) Kim, D. S.; Ozawa, T. C.; Fukuda, K.; Ohshima, S.; Nakai, I.; Sasaki, T. *Chem. Mater.* **2011**, *23*, 2700.
(28) Xu, Y.; Bai, H.; Lu, G.; Li, C.; Shi, G. *J. Am. Chem. Soc.* **2008**, *130*, 5856.
(29) Wu, Q.; Xu, Y.; Yao, Z.; Liu, A.; Shi, G. *ACS Nano* **2010**, *4*, 1963.
(30) Ong, E. W.; Eckert, J.; Dotson, L. A.; Glaunsinger, W. S. *Chem. Mater.* **1994**, *6*, 1946.
(31) Chang, K.; Chen, W. *ACS Nano* **2011**, *5*, 4720.
(32) Lv, W.; Tang, D. M.; He, Y. B.; You, C. H.; Shi, Z. Q.; Chen, X. C.; Chen, C. M.; Hou, P. X.; Liu, C.; Yang, Q. H. *ACS Nano* **2009**, *3*, 3730.
(33) Song, L.; Ci, L.; Gao, W.; Ajayan, P. M. *ACS Nano* **2009**, *3*, 1353.
(34) He, Q.; Wu, S.; Gao, S.; Cao, X.; Yin, Z.; Li, H.; Chen, P.; Zhang, H. *ACS Nano* **2011**, *5*, 5038.
(35) Lee, Y.; Bae, S.; Jang, H.; Jang, S.; Zhu, S. E.; Sim, S. H.; Song, Y. I.; Hong, B. H.; Ahn, J. H. *Nano Lett.* **2010**, *10*, 490.
(36) Kim, T. Y.; Lee, H. W.; Stoller, M.; Dreyer, D. R.; Bielawski, C. W.; Ruoff, R. S.; Suh, K. S. *ACS Nano* **2010**, *5*, 436.
(37) Meng, C.; Liu, C.; Chen, L.; Hu, C.; Fan, S. *Nano Lett.* **2010**, *10*, 4025.
(38) Stoller, M. D.; Park, S.; Zhu, Y.; An, J.; Ruoff, R. S. *Nano Lett.* **2008**, *8*, 3498.
(39) Qu, D. *J. Power Sources* **2002**, *109*, 403.